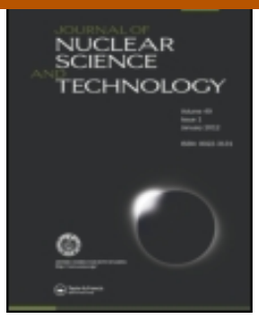

Journal of Nuclear Science and Technology

ISSN: 0022-3131 (Print) 1881-1248 (Online) Journal homepage: https://www.tandfonline.com/loi/tnst20

Application and In-depth Assessment of RETRAN-3D for Best Estimate Analysis of Nuclear Power Plant Transients

Paul CODDINGTON , Rafael MACIAN , Martin A. ZIMMERMANN & Rakesh CHAWLA

To cite this article: Paul CODDINGTON , Rafael MACIAN , Martin A. ZIMMERMANN & Rakesh CHAWLA (2002) Application and In-depth Assessment of RETRAN-3D for Best Estimate Analysis of Nuclear Power Plant Transients, Journal of Nuclear Science and Technology, 39:9, 972-985, DOI: 10.1080/18811248.2002.9715284

To link to this article: https://doi.org/10.1080/18811248.2002.9715284

Published online: 07 Feb 2012.

Journal of NUCLEAR SCIENCE and TECHNOLOGY, Vol. 39, No. 9, p. 972–985 (September 2002)

TECHNICAL REPORT

Application and In-depth Assessment of RETRAN-3D for Best Estimate Analysis of Nuclear Power Plant Transients

Paul CODDINGTON[1,*], Rafael MACIAN[1], Martin A. ZIMMERMANN[1] and Rakesh CHAWLA[1,2]

[1]*Paul Scherrer Institut, CH-5232 Villigen PSI, Switzerland*
[2]*Swiss Federal Institute of Technology (EPFL), CH-1015 Laussane, Switzerland*

(Received December 17, 2001 and accepted in revised form July 2, 2002)

The code RETRAN-3D has been extensively applied in the project STARS at PSI to perform BE analysis for a range of operational and other (non-LOCA) transients for the Swiss NPPs, which include both PWRs and BWRs. Extensive assessment employing experimental and plant data has provided confidence in the applicability and accuracy of RETRAN-3D for the analysis of transients in both types of LWRs. In this context, this paper presents an in-depth study of the performance of the code for two types of applications. First, a detailed analysis of BWR/6 recirculation pump trip tests shows that the code is able to accurately predict the coupled neutronic and thermal-hydraulic behaviour during an operational transient in which plant-specific system features (*e.g.* SRI insertion, response of the recirculation line valves to changes in flow, *etc.*) play an important role. Second, RETRAN-3D is applied to BE analysis of a PWR beyond-design basis scenario, namely the failure of the RHR system during reactor shutdown. In-depth assessment of the results obtained demonstrates the applicability of RETRAN-3D and the need for employing a BE approach to predict a more accurate, shorter "time window" for operator remedial action than that estimated using the assumption of uniform primary temperature distribution.

KEYWORDS: RETRAN-3D, best estimate, BWR type reators, PWR type reators, RHR type reactors, operational transients, shutdown analysis, nuclear power plants, performance, estimate analysis

I. Introduction

The project STARS (Safety research related to Transient Analysis of Reactors in Switzerland) represents a collaborative R&D effort between the Paul Scherrer Institute (PSI) and the Swiss Federal Nuclear Safety Inspectorate (HSK). Its basic mission is to provide an accurate deterministic safety assessment of the Swiss nuclear power plants (NPPs), consisting of 2 boiling water reactors (BWRs) and 3 pressurized water reactors (PWRs).

The system code RETRAN-3D[1)] is one of the main tools utilised to perform best estimate (BE) analysis for a range of operational and other (non-LOCA) transients for the Swiss LWRs. In accordance with the scope of the project, it has been necessary to demonstrate that this code is capable of calculating transients in which (a) a realistic representation of plant-specific features is important, and (b) conditions beyond those of traditionally considered operational events are encountered. Various aspects of the code's BE qualification have been considered in the process, including basic model development[2)] as well as assessment against separate effects measurements,[3–5)] and comparison of calculation results with integral experiments.[6)] This effort has provided confidence in the applicability and accuracy of the code for the analysis of transients in both types of LWRs.

It is in this context that this paper presents an in-depth study of the performance of RETRAN-3D for two specific types of applications to BWR and PWR plants. First, a detailed analysis of certain BWR/6 tests, *viz.* double and single recirculation loop pump trips, shows, by comparison of the results with plant data, that the code is able to accurately predict the coupled neutronic and thermal-hydraulic behaviour during an operational transient, in which plant-specific system features (*e.g.* Selected Rod Insertion (SRI), response of the recirculation line valves to changes in flow, *etc.*) play an important role.

The second aspect considered is the application of RETRAN-3D to a "beyond-design-basis" event. In this context, a study is presented of the primary system thermal-hydraulic behavior after the failure of the Residual Heat Removal (RHR) system during a PWR shutdown, which may lead to an over-pressurization of the reactor coolant system (RCS). The hypothetical scenario takes place with the system at 150°C and 25 bar. The thermal expansion of the primary inventory swells the RCS inventory until it becomes completely filled with liquid water. Further expansion of the liquid rapidly increases the RCS pressure, and there is concern that a break may occur. In-depth assessment of the results obtained shows the applicability of RETRAN-3D for these kinds of shutdown scenarios at relatively low temperatures and pressures, and the need for employing a BE approach to predict a more realistic system pressure response and a shorter "time window" for operator remedial action than that estimated using the simplifying assumption of *uniform* primary side temperature (perfect primary inventory mixing).

II. Analysis of BWR/6 Recirculation Pump Trip Transients

In order to have confidence in the application of a code to perform realistic (best-estimate) analysis of transients for an NPP, it is necessary to have both a well validated code and a comprehensive and validated input description of the plant in question. This input model should not only consider the

*Corresponding author, Tel. +41-56-310-2738, Fax. +41-56-310-2327, E-mail: Paul.Coddington@psi.ch

correct geometric representation of components, but also include a model of the plant control and protection system and, when necessary, a detailed representation of the reactor kinetics. In order to assess this "complete" plant-specific input description, it is usual to validate it in combination with the code against plant transient data. In this section, we present the results of the assessment of RETRAN-3D against two BWR/6 1,145 MWe (3,140 MWth) transients, *i.e.* a double and a single recirculation pump trip.[7] The calculations were performed with the Four-equation Dynamic Slip model because of its more numerically robust behavior in BWR analysis applications when compared to the Five-equation model described in Ref. 2).

The application of RETRAN-3D to the considered BWR plant start-up tests requires the use of an adequate modelling of the reactor kinetics. While RETRAN-3D has the option to use point kinetics (0-D), 1-D and 3-D kinetics, the use of point kinetics is not applicable here because of the transient changes in the axial power shape. In addition, the 3-D kinetics model for transient applications is still subject to a basic evaluation.[8] As a consequence, the 1-D kinetics model has been considered to be the most appropriate for application to the current analysis. The 1-D kinetics cross-sections were derived from CASMO SIMULATE[9] core-follow calculations using the cross-section radial homogenization code SLICK.[10,11] Following this procedure, cross-sections representative of the individual reactor fuel cycles were generated for the analysis.

The RETRAN-3D nodalisation of the reactor vessel is presented in **Fig. 1** and shows the lower plenum (control volumes 170 and 160), the upper plenum (150 and 140), with the core region lying between these two regions, the steam water separator (130 and 120), the steam dome (110 and 100), and the downcomer region (500 to 570). The feedwater enters the vessel at control volume 530 and the steam flows out into the steam line from control volume 500. The steam line nodalisation models each one of the four steam lines separately, each one with its own safety relief valves. Following the header, these lines are combined in the model into a single one which directs the steam to either the turbine inlet or to the condenser *via* the by-pass valve.

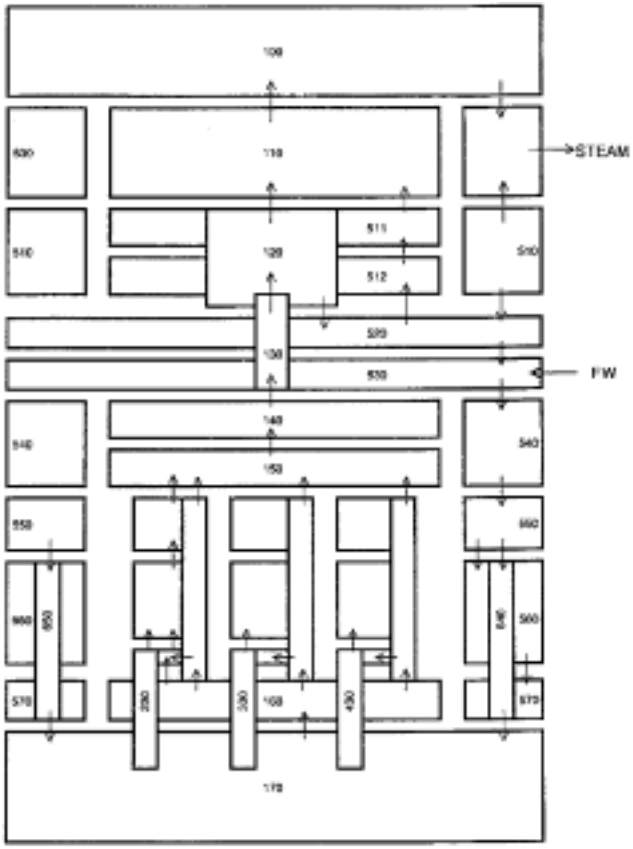

Fig. 1 RETRAN-3D BWR/6 vessel nodalization

1. Double Recirculation Pump Trip

(1) Transient Description

The trip of both recirculation loop pumps results in an immediate loss of pump head as the pump speed decreases, with a consequential loss of core flow and therefore core power. As the pump head decreases the vessel flow continues due to natural circulation with the driving head coming from the fluid density (void) difference between the core and upper plenum, and the downcomer. As the core flow and therefore power falls the reduction in steam flow produces a decrease in the pressure drop along the steam line with a consequential reduction in the reactor pressure vessel pressure. As a result of the reduction in the power and therefore steam flow, the plant feedwater controller responds to maintain a constant vessel water level. After about 20 s, when the recirculation loop pumps have coasted down, the vessel flow is just due to natural circulation, and under these conditions the plant reaches an equilibrium state with a core flow of about 30% and a core power of between 35% and 40% of the full power value. In order to eliminate the possibility of this final point lying within the unstable operating region, a group of 8 pre-selected control rods is inserted into the core once the speed of both pumps falls below 15% of the normal operating value. This selected control rod insertion (SRI) lowers the core power to about 30% and reduces the core flow to about 25%, thus producing a natural circulation state away from the BWR unstable region on the power *vs.* flow map.

Viewed in more detailed terms, the pump speeds decrease, following the trip of both recirculation pumps and the flow-controller, sensing the pump trips, locks the Flow Control Valves (FCVs) at their current positions. The immediate resultant decrease in the recirculation loop flows (Fig. 2) reduces the jet pump drive flows, resulting in a core flow decrease (Fig. 3). As a consequence, the "average core void" increases, which causes the core power (Fig. 4) to decrease immediately. This, in turn, results in a fall in the steam flow, causing the reactor pressure to drop (Fig. 5).

As a result of the decrease in core flow and consequent decrease in reactor pressure, the collapsed water level in the downcomer starts to rise, as indicated by the Narrow (Fig. 6) and Wide Range level measurements. The feedwater flow controller, which is regulated by both the steam flow and the downcomer level, responds to the reduced steam flow and increase in downcomer level to lower the feedwater flow after about 4 s. Once the total recirculation loop mass flow decreases below 1,750 kg/s, the recirculation loop flow con-

troller forces the FCVs to fully open according to the plant-specific event procedure.

As the reactor pressure stabilises, the feedwater flow rate keeps getting adjusted and the core void decreases, which causes the downcomer level to return back to its original value after about 25 s. After about 27.5 s after trip initiation when the pump speed falls below 15%, the plant core power drops rapidly due to the insertion of pre-selected control rods (Selected Rod Insertion, SRI). This plant-specific feature was included in the RETRAN-3D model.

It should be noted that the abrupt reduction in the observed recirculation loop drive flow after 30 s, seen in (Fig. 1), is a consequence of the instrumentation going "out of bounds" and is not an indication of the plant behaviour.

(2) Code Comparison against Plant Data

The comparison between the RETRAN-3D calculation and the plant data indicates very good overall agreement, and shows that the calculation was able to capture the main features of the test, including those that require feed-back from the plant control system.

The RETRAN-3D calculated reduction in the recirculation loop drive flow (**Fig. 2**), following the recirculation pump trip, shows that the initial flow reduction in the plant is observed to lag behind the calculated value. This results from a time delay in the plant signal of between 1 and 2 s, which was not included in these calculations. After about 6 to 8 s, *i.e.* when the flow has fallen to below about 50%, there is a consistent overprediction of the calculated value of the recirculation loop drive flow. It is possible that this occurs because of the following: As was noted above, in this particular plant the flow controller requires the FCVs to open fully as the recirculation flow rate falls below a certain value. This identifies a limitation in the plant model in the ability to correctly characterise the flow losses in the FCVs as a function of relative position.

The calculated reduction in the core flow that accompanies the fall in the jet-pump drive flow is shown in **Fig. 3**. Again, the initial reduction is well predicted once an allowance is made for the time delay of up to 2 s in the plant signal. However, there is a difference between the calculated and measured values after about 8 to 10 s. We see that the RETRAN-3D results overpredict the plant data in a manner consistent with the overprediction of the jet pump drive flow.

The initial decrease in the core power (**Fig. 4**) is well predicted by the RETRAN-3D calculation. After about 2 to 3 s, the core power is overpredicted, and the degree of overestimation remains almost constant after about 10 s as the rate of the core flow reduction strongly decreases. During the first 10 s, the plant data shows a more rapid reduction in the power, following the initial core flow runback and increase in core void, with a small recovery as the fuel temperature falls and the core Doppler reactivity increases. In the calculation, the power reduction has a smoother response, most likely as a consequence of the different core thermal time-constants.

There are several different phenomena that determine the core power response following the core flow reduction, *e.g.* magnitude of void increase, dependence of reactor cross-sections on moderator density and fuel temperature, and change in average fuel temperature as a function of the change in power. While it is found that the calculated net core flow reduction (Fig. 3) is slightly smaller after 10 s, it is likely that major reasons for the power difference are an underprediction in the change in the core average void and a different thermal response of the core, *i.e.* change in the average fuel temperature, as the core power reduces. It is, for example, difficult to match the combined response of the many reactor fuels pins with just one representative calculational pin without careful "tuning".

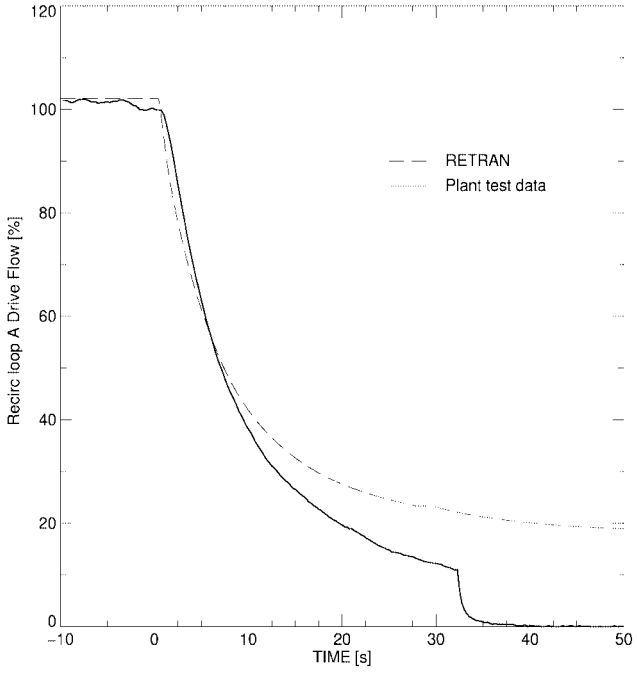

Fig. 2 Recirculation loop drive flow (Double recirculation pump trip)

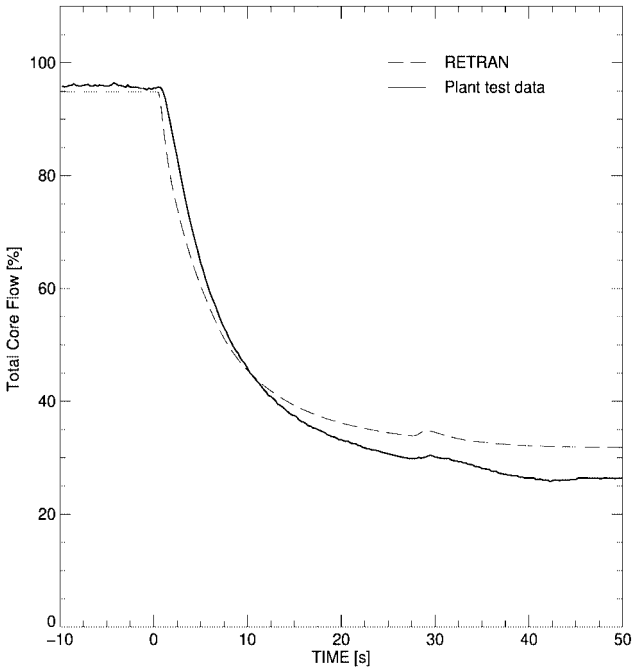

Fig. 3 Total core flow (Double recirculation pump trip)

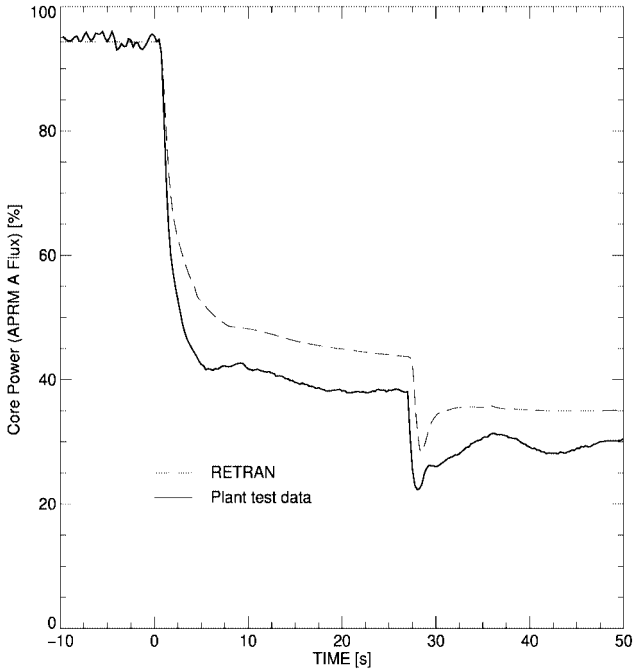

Fig. 4 Core power (Double recirculation pump trip)

The rapid power reduction in the power that follows the SRI at about 27 s is well predicted by the RETRAN-3D calculation.

The comparison of the change in the calculated and measured steam dome pressure given in **Fig. 5** shows very good agreement, both for the initial reduction in power and that following the selected control rod insertion. This confirms both the ability of the RETRAN representation of the plant controller to predict the change in the turbine inlet pressure as a function of the steam flow, as well as a correct representation of the steam line pressure losses again as a function of the steam flow rate.

The prediction of the change in the measured Narrow (**Fig. 6**) Range water levels is good. The water level rises initially as the total core flow, and therefore the downcomer flow, fall. The plant data shows an increase in the narrow range water level of about 20 cm whereas the calculation gives a value of about 30 cm. Again the plant response appears to be slower because of a time delay in the observed signal of between 1 and 2 s. After about 5 s the level begins to fall as the feedwater flow is reduced to compensate for the reduction in the core power (in fact it is the sensed steam flow that is used in the feedwater controller) and the increase in the water level. Eventually, *i.e.* after about 20 to 25 s, the feedwater controller brings the downcomer level back to close to its original value. There is a rapid reduction in the level following the SRI at about 27 s in both the plant data and the RETRAN-3D calculation, with a minimum in the level of about −25 cm occurring in both the calculation and the plant data at about 36 to 38 s. Following this minimum, the feedwater controller in the plant brings the level back to its original value, while in the RETRAN model for these low power conditions, the feedwater response is much slower.

After about 10 s, when the pressure has stabilised, the calculated steam flow is higher than the plant measurement confirming the higher calculated core power and hence underlining the "self-consistency" of the comparisons.

2. Single Recirculation Pump Trip Test

(1) Transient Description

This transient test was performed to examine the plant behaviour under asymmetric flow run-down conditions. The

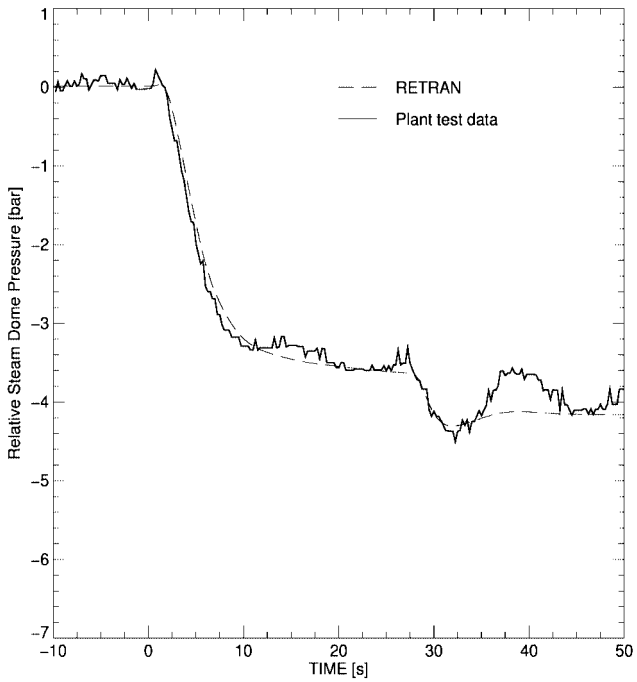

Fig. 5 Relative steam dome pressure (Double recirculation pump trip)

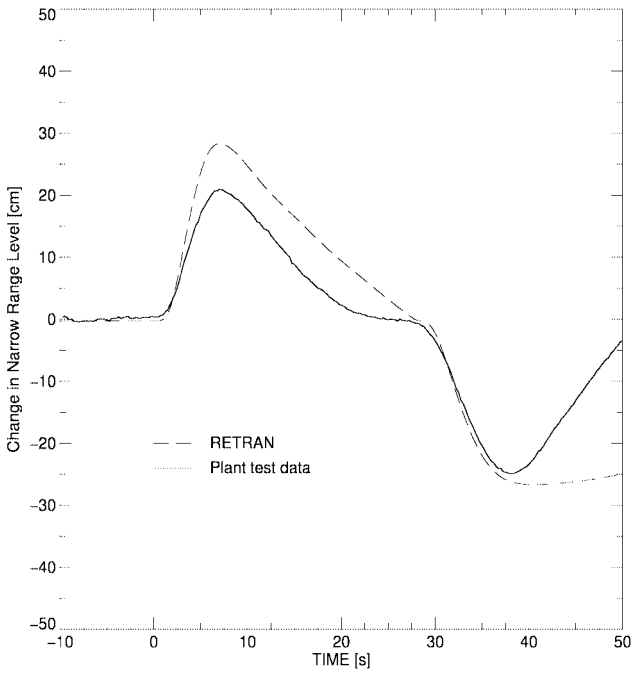

Fig. 6 Narrow range downcomer water level (Double recirculation pump trip)

trip of a single recirculation loop pump results in a reduction in the total core flow which, because of the non-linear dependence of pressure drop on flow, decreases the vessel flow pressure drop and so increases the flow through the jet pumps connected to the untripped recirculation pump. The pressure drop across the jet pumps resulting from the continued operation of one of the two recirculation loops produces first a stagnation and then a reversal of the flow through the jet pumps connected to the tripped loop. For this test, therefore, the final core flow comes from the sum of positive flow through the jet pumps connected to the untripped loop and the negative flow through those connected to the tripped loop. The ability to successfully calculate this transient requires an accurate representation of the jet pump losses for both forward (at up to 150% of normal flow) and reverse flow conditions.

In more detailed terms, following the trip in the recirculation pump A, the pump speed decreases producing a fall in the recirculation Loop A drive flow (**Fig. 7**) while the recirculation loop flow-controller locks the FCV A at the current position. It should be noted that similarly to the double recirculation pump trip, the abrupt fall in the Loop A flow at ∼23 s occurs because the instrumentation goes out of range and is not indicative of the plant behaviour. The pump speed in Loop B stays more or less constant, and the flow-controller starts to throttle FCV B after about 4 s due to the continuous increase in drive flow. The increase in the drive flow in the operating loop (Loop B) comes from the reduction in the total loop flow resistance, which follows from the reduction in the loop A flow and therefore the total core flow (**Fig. 8**).

The total core flow for the plant, shown in Fig. 8, is obtained from the sum of the flow through the two individual jet pumps. The jet pump flow is obtained from a measurement of the pressure drop. This has two consequences, *viz.* a loss of accuracy at low values and the fact that a positive flow is indicated irrespective of the sign of the pressure drop. This results in the observed increase in the plant core flow after about 12 s as the flow through the jet pumps attached to the tripped loop first stagnate and then reverse. If the plant protection system senses a trip in only one of the two recirculation pumps and if the pump speed falls below 15% of its original value, then the data acquisition system subtracts the loop flows. This can be seen to occur after about 25 s in Fig. 8 when the core flow falls abruptly to about 57%. After about 25 s, the core flow slowly decreases to a value of about 50%.

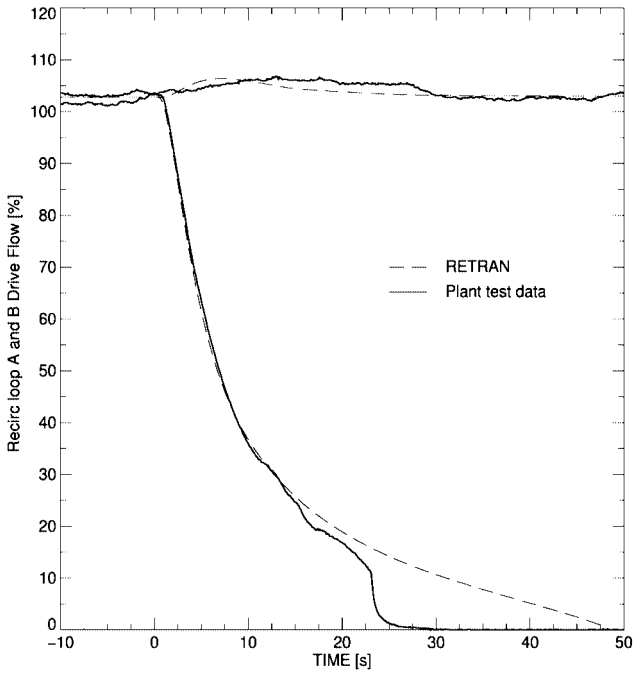

Fig. 7 Recirculation loop A and B drive flow (Single recirculation pump trip)

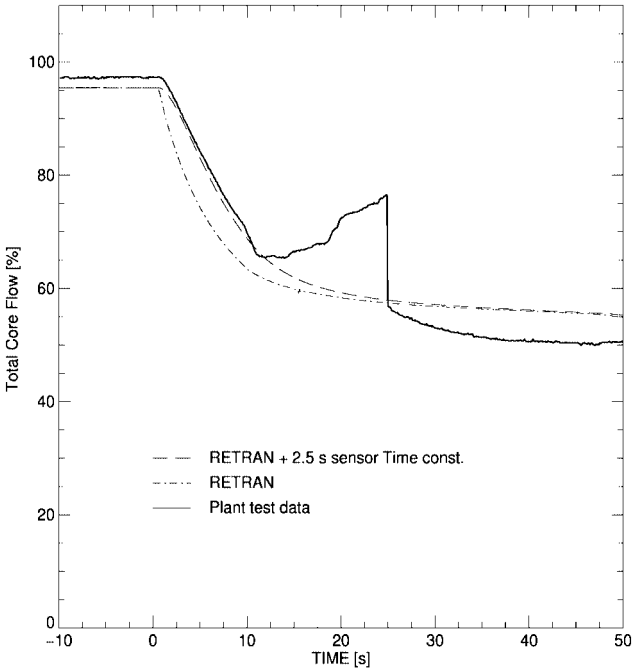

Fig. 8 Total core flow (Single recirculation pump trip)

The reduction in the core flow produces an increase in the core average void and therefore an immediate drop in core power (**Fig. 9**). The core power falls to about 65% of its initial value compared to about 40% in the case of the double pump trip. The core power decrease leads to a continuous reduction in steam flow, which causes the reactor pressure to fall. The core flow appears to fall slower than would be suggested by the rapid fall in the core power. This results from a sensor time constant in the process core flow signal of up to 2.5 s. The Narrow and Wide Range water levels behave in a very similar way, during the first 20 s, to that observed in the Double Recirculation Pump Trip test. The narrow range level presented in **Fig. 10** shows an increase of about 10 cm, which is about half that of the double recirculation pump trip test and is consistent with the slower reduction in the core flow.

(2) Code Comparison against Plant Data

As in the case of the Double Recirculation Pump Trip test, the calculations performed with RETRAN-3D, when compared against the plant data, show good overall agreement for this transient. The prediction of the loop A drive flow (tripped loop) shown in Fig. 7 would appear to be better than that for the double recirculation loop trip, and this is, at least in part, do to the fact that for this transient the FCV position in loop

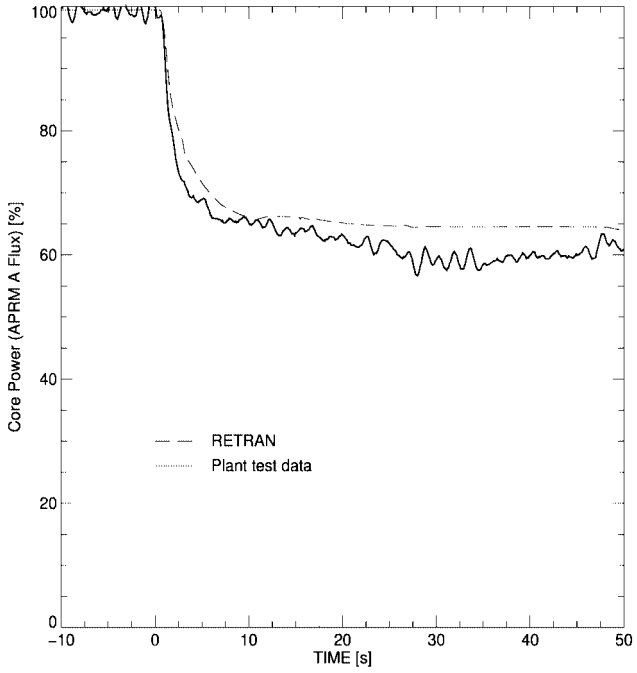

Fig. 9 Core power (Single recirculation pump trip)

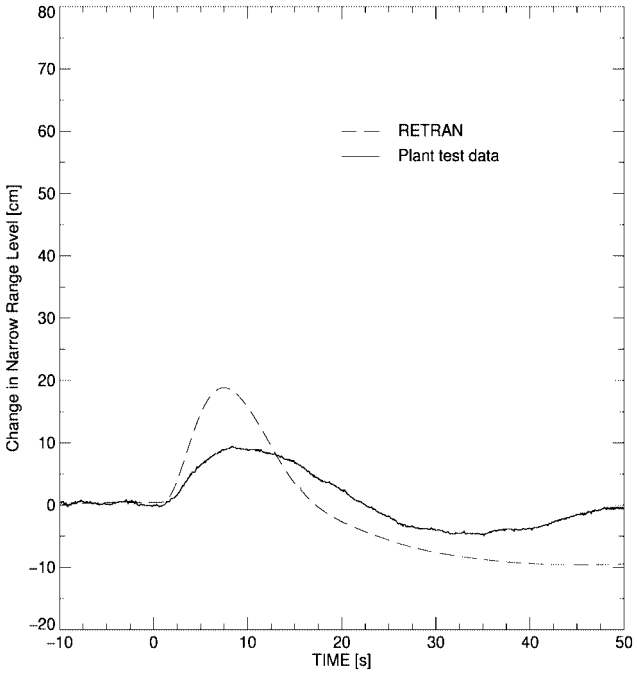

Fig. 10 Narrow range downcomer water level (Single recirculation pump trip)

A does not change.

The calculated total core flow is well predicted for the first 10 seconds, Fig. 8 showing the results of the RETRAN calculation with and without the 2.5 s sensor time constant. The accurate prediction of the core flow produces a good prediction of the core power during this initial period (Figs. 7 and 9). Between about 12 and 25 s when the plant data indicate an increase in the core flow, it is difficult to make a detailed comparison. However, the indications from both Fig. 8 and the core power (Fig. 9) are that the RETRAN-3D calculation slightly overestimates the core flow and hence the core power.

After about 20 s, the calculated core power reaches a plateau of about 65%, compared to a plant value of about 60%, and the core flow a calculated value of 55% compared to the plant value of about 50%. In this respect, the comparison is similar to that of the double recirculation loop pump trip, in that both calculations consistently overpredict the core flow and reactor power under reduced flow conditions. This would imply that the calculated low-flow vessel pressure drop is being under-estimated.

The prediction of the change in the downcomer water level (Fig. 10) is of a similar quality to that for the double recirculation pump trip. Again, both calculations overpredict the initial (0 to 10 s) increase in the water level as the downcomer flow decreases. Since the initial change in the total core flow is well predicted (Fig. 8), the cause for the discrepancy most probably lies with the change in the separator inventory as the core flow is reduced. In both cases, the separators are modelled in a quasi steady-state manner. After the initial increase in the downcomer level, the feedwater controller reduces the feedwater flow to bring the level back to its original value after about 25 to 30 s.

As with the calculation of the double recirculation pump trip transient, the degree of agreement with plant data is quite consistent with results reported elsewhere, *e.g.* for RETRAN-02[12] and RETRAN-03[13] analyses of BWR/5 tests.

3. Summary

The following BWR/6 transient tests have been analysed using RETRAN-3D: Double Recirculation Pump Trip and Single Recirculation Pump Trip.

Generally, the calculations show a good overall agreement with the plant data. Both models are able to capture the main features of the two transient tests, and the main thermal hydraulic variables show excellent agreement between the code predictions and plant measurements.

For the double recirculation pump trip test, it has been possible to capture the transition from forced to natural circulation flow around the vessel. Although the reduction in the recirculation pump speed is accurately calculated, there is a consistent overprediction of the recirculation loop drive flow under low flow conditions due to the lack of data to of accurately model the flow resistance of the FCVs as a function of position. Following the establishment of natural circulation vessel flow, the total core and, therefore, core power is overpredicted by RETRAN-3D.

For the BWR/6 considered, following a trip of both recirculation pumps, the plant-specific event procedures require the insertion of a select number of control rods (SRI) in order to ensure that the natural circulation point (power *vs.* flow) is well separated from the unstable operating region. In order to model this particular plant feature, cross section sets were required for multiple control states. The power reduction that followed SRI, which was initiated automatically when the pump speed fell below 15%, was well calculated.

For the single recirculation pump trip test, the flow through the jet pumps attached to the untripped loop increases, while the flow through those attached to the tripped loop initially

stagnates and then reverses. With the total core flow being the sum of these two flows, accurate predictions for this test require a good representation of the plant jet pump operation under a wide range of forward and reverse flow conditions. The initial reduction in the core flow is well modelled. The final core flow and consequently the core power are slightly overpredicted. However, the prediction is better than that for the double recirculation pump trip test. Generally, the system losses require improved modelling, particularly those for the jet pump, under conditions away from normal operation.

III. Analysis of Thermal Expansion during Shutdown in a PWR

In this section, we examine the application of RETRAN-3D to the best estimate analysis of a beyond design basis transient. The study considers the consequences following the hypothetical failure of the Residual Heat Removal (RHR) system during shutdown in a Pressurized Water Reactor (PWR). If the RHR system decay heat removal capability cannot be ensured, then the decay heat released in the core will heat up the Reactor Coolant System (RCS) inventory and will cause it to expand. If the thermal expansion is such that the entire RCS becomes completely filled with water, then further expansion will result in a rapid increase of the RCS pressure. Such a situation could threaten the integrity of the RCS pressure boundary and lead to a dangerous break in the primary system or in the lines of the systems connected to it, *e.g.* the RHR system.[14] The pressure increase can be arrested by the opening of the pressurizer relief valves (PORVs), or in those PWRs in which the RHR system is not isolated after it fails, by the opening of the pressure relief valve in the RHR system line.

The purpose of the analyses presented in this section is to determine whether mitigating measures, such as the opening of one of the PORVs and the RHR relief valve, are capable of preventing a fast pressure increase. A best estimate analysis of this scenario has been performed using RETRAN-3D for a typical two-loop Westinghouse-type PWR. The analysis considered the shutdown state of the plant in which the conditions are most severe from the point of view of decay heat and RCS configuration. Two cases have been analyzed, namely a Base Case with the pressurizer initially half-full, and a more conservative case with the pressurizer initially full.

1. Initial Conditions

The severity of the thermal expansion scenario depends on the decay heat level and on the RCS configuration (inventory, temperature, pressure, *etc.*) at the time of the RHR system failure, since these determine the speed at which the RCS inventory expands and the RCS pressure increases after the RCS fills completely.

For the reference PWR used in this analysis, a two-loop 1,130 MWth Westinghouse-type PWR, the worst case scenario, according to previous shutdown risk analyses, occurs at the beginning of the shutdown configuration at 22.4 h after shutdown, with a decay heat power level of 0.675% nominal full power. The RCS is then highly subcooled ($\Delta T_{\text{subcool}} \sim 74$ K) and at low pressure (~16% of nominal operating pressure.) The RCS is full of liquid with the pressurizer level reaching half its height. The RCS pressure is maintained by keeping the fluid in the pressurizer at saturation conditions for the RCS system pressure with the help of the pressurizer heaters (switched off once the scenario begins.) A small flow is maintained in the RCS by running one of the reactor coolant pumps (RCPs) in order to provide flow to the RHR for removal of the decay heat. This pump is tripped after the RHR fails (the initiator event of the scenario.)

The secondary sides of the steam generators are isolated and at saturation in thermal equilibrium with the primary side. They are assumed to remain isolated during the scenario, so that their role as a sink of decay heat is not enhanced by venting steam to the condenser. The secondary side inventory in this configuration contains ~34% of the total system mass (primary and secondary.)

In the reference PWR there are three PORVs, but only one of them has its opening set-point reduced during the shutdown mode of operation to provide overpressure protection at the low shutdown pressures. For this reason, only the PORV with the lowered opening set-point was assumed to be activated during the scenario, although the other two PORVs can be opened by the operator at any moment. The mass flow rates of the open PORV and RHR relief valve are assumed to be the minimum under the critical flow conditions present during the scenario, as given by the valves' manufacturers specifications. In reality, the increase of RCS pressure and the change of thermodynamic conditions should determine the actual critical flow through the valves. In order to provide a bounding estimate of the RCS pressure behavior and conclusions, it was decided to adopt the minimum flow values for the entire transient.

2. Description of the RETRAN-3D Model

Data from a two-loop 1,130 MWth Westinghouse-type reference PWR were used to develop the RETRAN-3D input model (see **Fig. 11**). The detailed system model includes the pressure vessel and its internals, the pressurizer and surge line, the steam generators with the secondary sides, the pumps, and the cold and hot leg lines. The metal masses in the primary system, vessel, core and steam generators were also taken into account. The pressurizer is connected to Loop A and the RHR system injection and suction points (modelled as two FILLS) are attached to the cold and hot legs of Loop B, respectively. The RHR lines are isolated during the transients. The initial water inventory and thermodynamic conditions in the secondary sides are adjusted according to the initial conditions expected at the beginning of the scenario. A power-*vs.*-time table simulates the decay heat and is based on a decay heat formula for the reference PWR end-of-equilibrium-cycle conditions. This formula yields a higher decay heat level (~25%) than the standard ANS-79.[15] Thus, the time windows for operator action to prevent a dangerous system pressurization above the RHR design limit (1.9 MPa above RHR operating pressure) obtained in the calculations shown below are expected to be shorter than if the ANS-79 decay heat standard had been used.

The main initial steady-state parameters are displayed in **Table 1**. The pressures have been normalized to the pressure

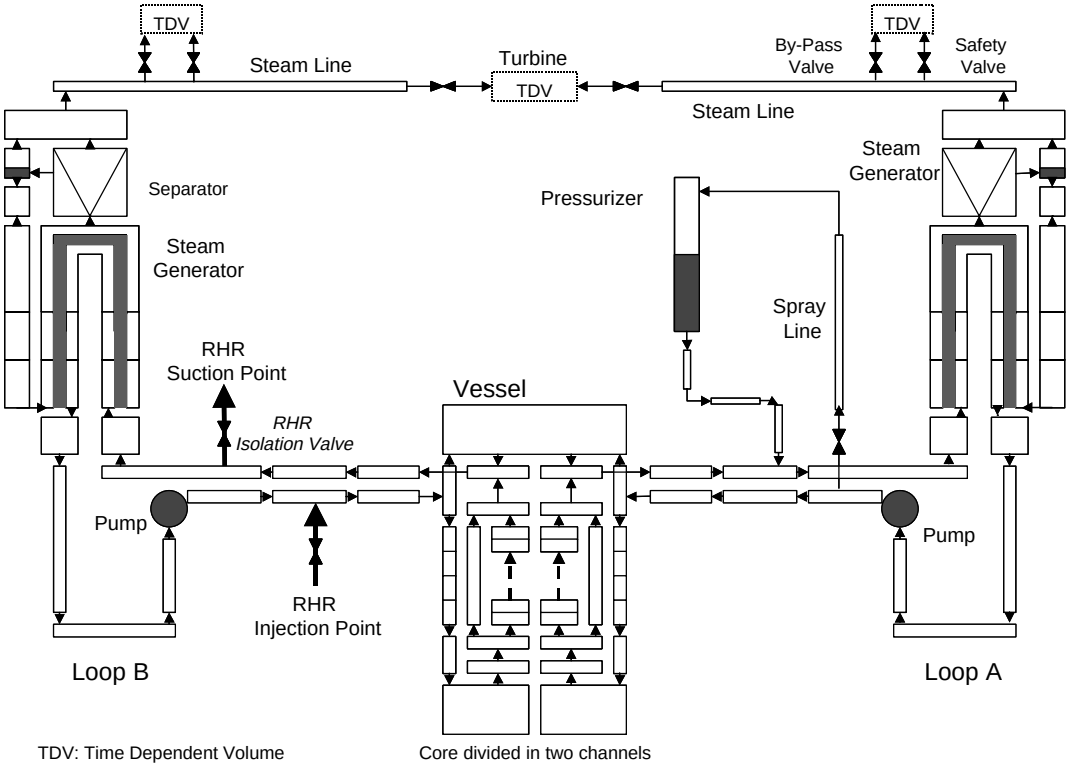

Fig. 11 RETRAN-3D 2 loop PWR system nodalization

Table 1 Initial system normalized parameters

Main system parameters	RETRAN-3D	Reference PWR
Initial decay heat power level	0.675% nominal	0.675% nominal
RCS Avg. hot leg subcooling	73.4 K	74.0 K
RCS normalized pressure[a)]	1.0	1.0 (16.12% nominal)
Secondary side normalized pressure[a)]	0.832	1.0 (8.5% nominal)
Total RCS normalized mass[b)]	0.993	1.0 (nominal 1/2przr.r)
Total secondary side mass (2SGs)	1.026	1.0
Total system mass (RCS+2SGs)[b)]	1.004	1.0

a) Normalization pressure is initial pressure at beginning of scenario.
b) Normalized value is mass at the beginning of scenario.

at the beginning of the scenario, and the masses to the initial inventories to permit a better comparison between the calculations and the reference values. The calculated primary side conditions are very close to the reference plant's conditions at the beginning of the thermal expansion scenario.

The water masses, which are important to determine the progression of the accident, since they act as heat sinks and expand, are also quite similar. The largest difference is about 2.6% for the secondary sides, while the total system masses differ by less than 0.4%. The difference in the secondary side pressures corresponds to about 7 K difference in saturation temperature. This was necessary, because RETRAN-3D had difficulties in achieving a steady-state solution with both the primary and secondary sides in thermal equilibrium.

3. Base Case

The base case started from the steady-state conditions presented in Table 1. Primary side inventory was only lost through one of the PORVs. The characteristics of this valve are an opening set-point for an overpressure of 0.57 MPa above the RCS pressure at the beginning of the scenario, with a delay of 3.45 s (0.75 s dead time +2.7 s activation), and a reseating set-point for an overpressure of 0.1 MPa, with the same delay. The minimum mass flow rate for the conditions expected during the scenario, selected as a conservative assumption (from manufacturer's data), is $5.39\times10^{-4}\,s^{-1}$, normalized to *total* initial RCS inventory, *i.e.* it would take about 0.5 h to empty the entire RCS if this valve would remain continuously open and vent at this rate. The only flow in the RCS was caused by natural circulation.

After the RHR system failure, the decay heat caused the fluid to expand, steadily increasing the pressurizer level. The RCS pressure, initially at 16.12% of *nominal* pressure, started to fall, reaching a minimum value 0.6 MPa lower than the initial pressure after about 1.75 h. The injection of substantially subcooled ($\Delta T_{subcool}$=73.4 K) RCS inventory into the

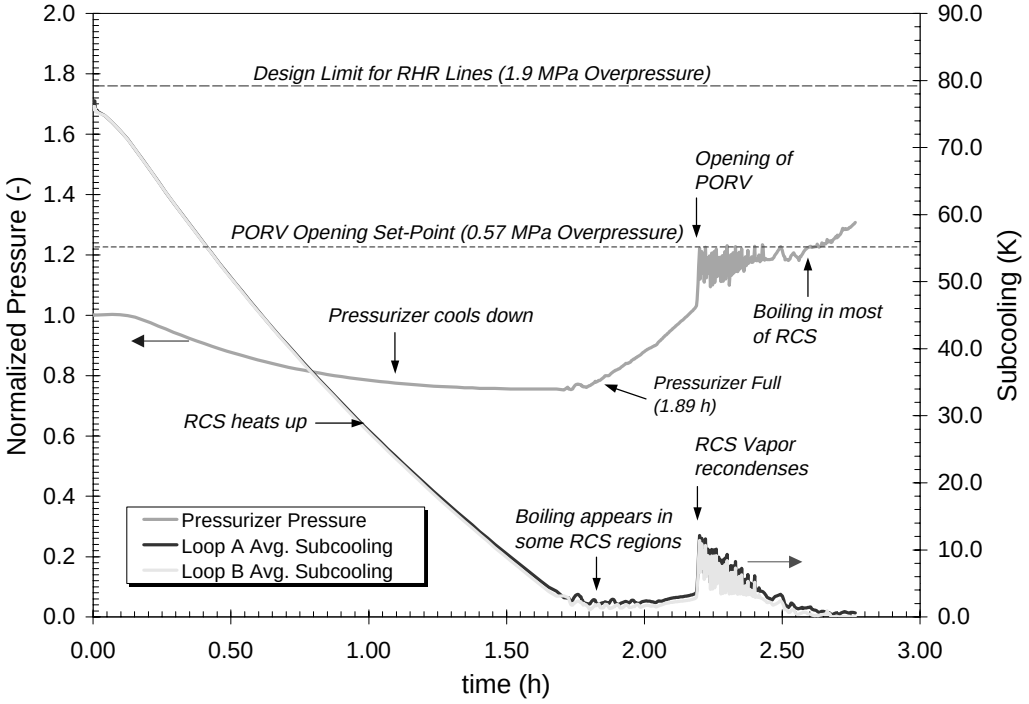

Fig. 12 Base case (Pressurizer pressure and average subcooling for loops A and B)

pressurizer (initially at saturation in order to maintain system pressure) decreased its temperature, and the steam (initially saturated) cooled down and condensed, thus reducing the RCS pressure. **Figure 12** shows how the average temperature of the fluid in the pressurizer steadily decreased as the subcooled condensate filled the pressurizer (the heaters were switched off at the beginning of the scenario.)

It is important to note that the decrease in system pressure predicted by RETRAN-3D may have been influenced by the fact that this code, like other one-dimensional thermal-hydraulic system analysis codes, tends to diffuse energy from one computational cell to another by reason of the numerical methods used, and it is difficult to simulate stratified temperature fields. In a real scenario, a stratification of cold and hot liquid layers may form, separated by a turbulent thermal mixing layer, which may result in the RCS pressure not decreasing as much as predicted.

After about 1.75 h, the pressurizer water level almost reached the top, and the compression of the steam bubble initiated a pressure increase. The continuing expansion of the RCS inventory eventually collapsed the steam bubble and the pressurizer became full of liquid at ∼1.82 h (see **Fig. 13**). After the level reached the top, it remained at its maximum value (9.62 m) for the remaining of the scenario. An additional calculation performed with a more refined noding scheme for the top of the pressurizer did not change this behavior.

By this time, void appeared in some locations of the RCS, *e.g.* the upper plenum (see **Fig. 14**), as the fluid reached saturation conditions. The pressure increase was thus 'cushioned' by the appearance of compressible vapor in the system. However, the increasing liquid expansion ultimately collapsed the void filling the RCS entirely with liquid at about 2.15 h. The RCS inventory continuing expansion caused its pressure to rapidly reach the PORV opening set-point at about 2.2 h.

A period of oscillatory pressure followed as the PORV opened and closed, thus keeping the RCS pressure below the PORV opening set-point up to about 2.6 h. Following this, a steady rise in RCS pressure is observed in Fig. 14. The explanation for the pressure rise above the PORV set-point can be found by studying Fig. 14. After 2.6 h, the RCS temperature in many locations reached the saturation value. As a consequence, the volumetric expansion (per unit of energy addition) of the RCS fluid increased to a value greater than the volumetric fluid (single phase liquid) loss through the open PORV. It is seen that this then leads to an increase in pressure.

A *stand-alone* calculation (based on thermodynamic principles) was carried out assuming that the entire RCS inventory is uniformly heated, so that, in this analysis system pressure exceeded the PORV pressure only after the entire RCS reached saturation. In the RETRAN-3D analysis, which can simulate the effects of the localized decay heat source in the core, of the natural circulation flow in the RCS, and of the metal masses and secondary sides in the RCS temperature distribution, the RCS pressure became greater than the PORV opening set-point *before* the entire RCS reaches saturation conditions. This can be explained by the fact that the fluid in the RCS was not at the same temperature and pressure everywhere. Thus, some regions, *e.g.* core, upper plenum and top of U-tube bundle, reached saturation and produced vapor, while most of the RCS remained subcooled. In **Fig. 15**, one can see this starting at ∼1.75 h, for which time RETRAN-3D predicts that some of the decay heat went into the heating up the RCS subcooled inventory and some into vapor production. It is important to note that Fig. 15 shows average subcooling referenced to the upper plenum pressure, meaning that, since the fluid out of the vessel is saturated, the incoming flow to

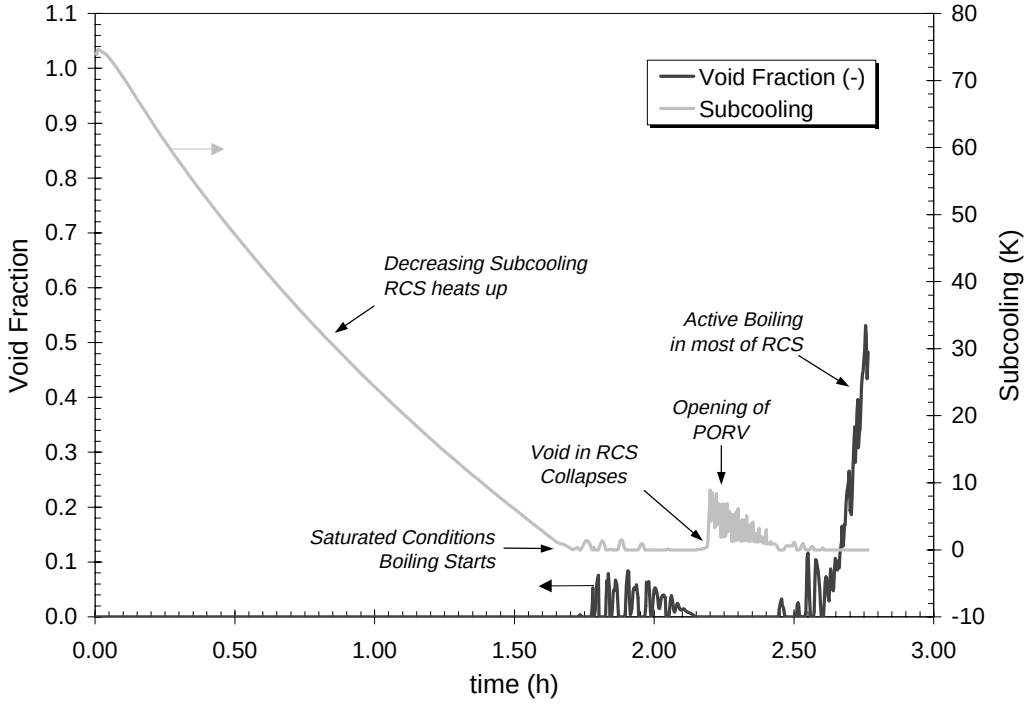

Fig. 13 Base case (Upper plenum subcooling and void fraction)

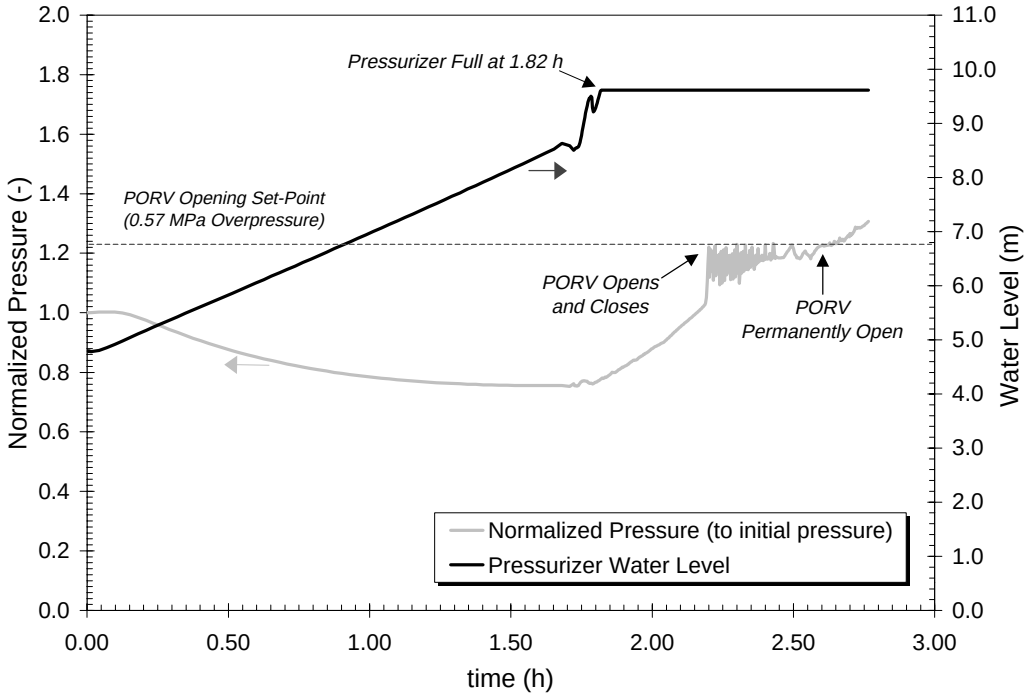

Fig. 14 Pressurizer water level and normalized pressure

the vessel must be subcooled after transferring heat into the steam generators.

The *stand-alone* calculation predicted that the entire RCS would reach saturation in ∼2.85 h (at about the same time (∼2.6 h) that the RETRAN-3D calculation predicted an *average* subcooling near zero). In reality, an entire RCS at saturation can never be achieved under the conditions of the scenario analyzed, since the increasing pressure due to the two-phase expansion, would increase the saturation temperature along the RCS, thus rendering the flow downstream of the steam generators subcooled. Thus, the best estimate code calculation, as a consequence of the ability to simulate the temperature distribution in the RCS, was able to capture this phenomenon and yielded a more realistic, and shorter, time window (2.6 h *vs.* 2.85 h) for operation action (defined as the time before the RCS pressure increases above the PORV set-

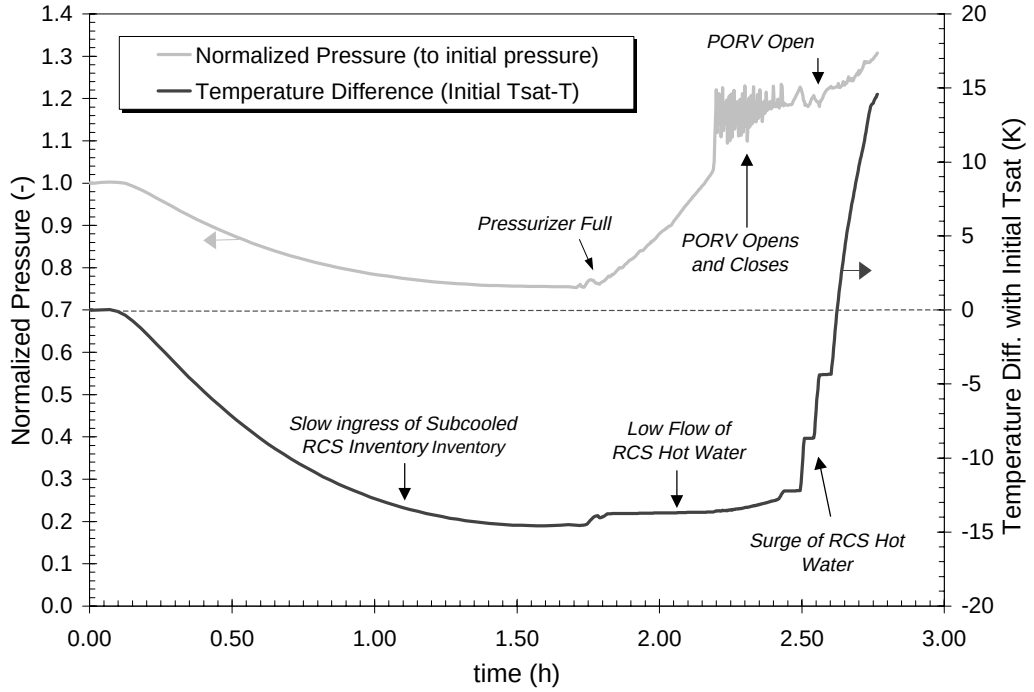

Fig. 15 Normalized pressurizer pressure and temperature difference

point) than otherwise would have been computed by assuming a uniform temperature throughout the RCS resulting from a perfect mixing of the primary inventory.

It is important to note that, although the above time difference between the stand-alone calculation (2.85 h) and the system analysis (2.6 h) is not large for this scenario, it may be so in other circumstances with other boundary conditions, *e.g.* different PORV flow rates.

The loss of RCS inventory through the now constantly open PORV and the compressibility of the system per unit of energy added, contribute to determine a rate of RCS pressure increase that prevents the RCS pressure from reaching the maximum pressure allowed for the RHR system (1.9 MPa overpressure above the RCS pressure at the beginning of the scenario) for a time significantly greater than 2.6 h (*i.e.* the time when the PORV becomes fully open). Unfortunately, further extension of the calculation was hindered by code convergence problems for highly voided, low pressure and power conditions. Thus, this analysis gives a time window of *at least* 2.6 h for operator action to restore some form of decay heat removal before the integrity of the RHR is challenged.

4. RCS Initially Full

Two additional thermal expansion scenarios have also been analyzed. They start with the failure of the RHR system 22.4 h after shutdown with the pressurizer completely full. The pressure starts a rapid increase a short time after the RHR system fails.

(1) Pressure Relief through the PORV

When the thermal expansion scenario started with the RCS filled with water, the RCS pressure rose very rapidly up to the PORV opening set-point, and a cyclic opening and closing of this valve followed. When the PORV opened, the RCS inventory was still highly subcooled ($\Delta T_{\mathrm{subcool}} \sim 73$ K), so that no void formation occurred. The loss of inventory through the PORV valve is then sufficient to compensate for the thermal expansion of the RCS inventory, which pushed coolant inside the pressurizer.

A *stand-alone* calculation of the rate of expansion of the RCS water, that took into account all the RCS and secondary sides water and metal masses, yielded a rate of expansion about 80 times lower than the volumetric flow rate through the PORV. Thus, a short valve opening time significantly reduced the RCS pressure, as shown in **Fig. 16**. The RCS pressure remained, therefore, below the PORV opening set-point while the temperature in the RCS remained below the saturation temperature (see Hot Leg A subcooling in Fig. 16).

As the fluid in many regions of the RCS (*e.g.* upper plenum, core, hot legs) reached saturation conditions, the fluid expansion became similar to that observed in the Base Case. The fact that this phenomenon appeared at roughly the same time in both cases ($\sim$2.6 h) occurs because the loss of energy per unit mass though the PORV flow is much smaller than the decay heat released to the RCS. The time window for operator action before the pressure steadily increased above the PORV set-point, therefore, depends mainly on the initial RCS subcooling ($\Delta T_{\mathrm{subcool}} \sim 73$ K) and on the ratio of decay heat *vs.* total system mass (0.041 MW/t).

Thus, the opening of only one pressurizer PORV appears to be able to hold the increase in RCS pressure below the PORV opening set-point, even when the thermal expansion scenario begins with the RCS completely full, while the RCS remains subcooled in most regions. The pressure rise caused by the expansion of the RCS inventory is thus kept within acceptable limits for at least 2.6 h. After this time, substantial vapor production in the RCS, together with the thermal expansion,

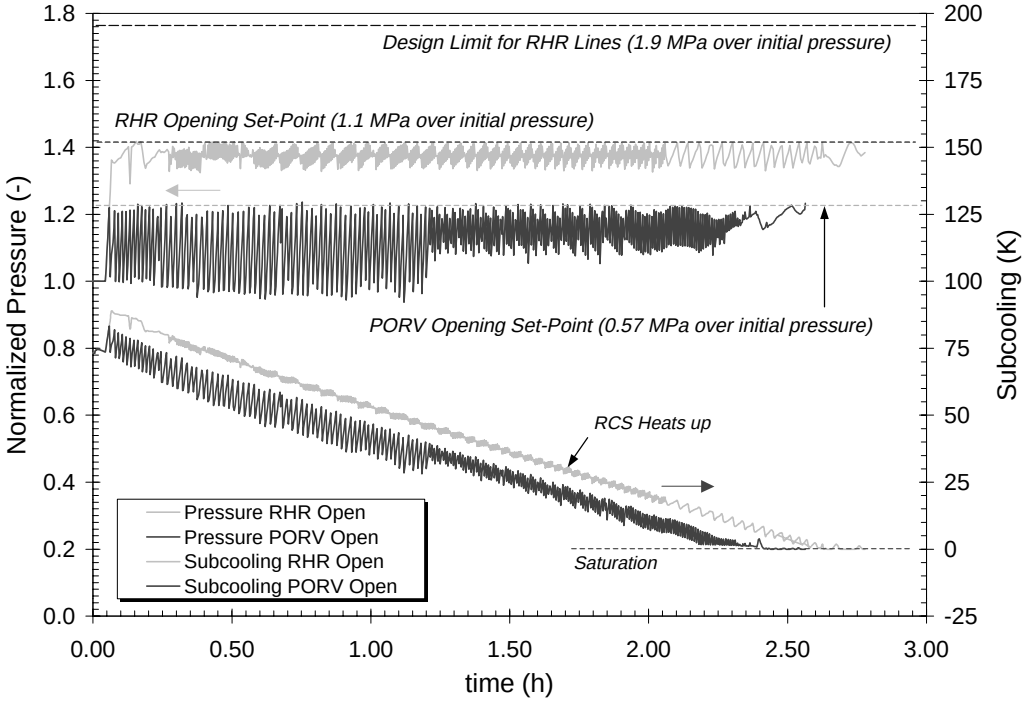

Fig. 16 RCS initially full (RCS normalized pressure and subcooling in hot leg A)

increases the RCS pressure in the same way that in the Base Case discussed earlier.

(2) Pressure Relief through the RHR Relief Valve

The second case with the RCS initially full assumed that the PORV failed to open. Under such conditions, only the RHR relief valve was available to limit the pressure increase. This scenario is not possible for those PWR plants which have, as an operating procedure in case of RHR failure, the isolation of this system.

The minimum mass flow rate assumed (from manufacturer's data) for the RHR relief valve under the scenario conditions is $9.22\times10^{-5}\,\mathrm{s}^{-1}$ (normalized to initial RCS mass; it would empty the RCS in ~3 h). The valve opening and closing set-points are respectively 1.1 MPa and 1 MPa above the pressure at the beginning of the scenario.

During the thermal expansion, the RCS pressure followed a similar behavior to that observed for the case of the opening of the PORV valve. The thermal expansion of the RCS liquid increased the RCS pressure rapidly until it reached the RHR relief valve opening set-point at about 0.08 h. From then on, the cyclic opening and closing of the valve maintained the RCS pressure below the RHR valve opening-set point (the same comments about the cycling opening and closing of the PORV mentioned earlier apply to this valve). The RHR valve provided a volumetric flow rate approximately 10 times larger than the rate of RCS volume thermal expansion mentioned above.

At about 2.75 h, the RCS systems started to void because the temperature in many locations reached the saturation value, and the RCS pressure started to rise above the opening set-point, similar to the two cases studied earlier. During this time, the maximum allowed pressure for the RHR lines was never reached. In summary, the RHR relief valve venting capacity appears to be enough to prevent the RCS pressure from reaching the RHR maximum allowed pressure for at least 2.75 h. The difference in time with respect to the two previous cases discussed above is caused by the higher system pressure, which implies a higher saturation temperature.

Finally, **Fig. 17** shows the initial seconds of the scenario for both cases with the RCS initially full. According to the figure, the rate of pressure increase after the system became 'water-solid' was about 0.11 bar/s. The PORV and RHR valves have a response time of about 3.5 s until fully open (typical values from manufacture's data). This gives a large time margin to avoid a very rapid pressure increase, similar to a pressure spike, even with the RCS initially full. Moreover, the increase of RCS pressure is linear, as can be expected from a thermal expansion process with a constant source of power.

According to the linear pressurization rate in Fig. 17, if *no* relief valve opened, it would take about 1,410 s to reach the RCS design limit (1.16 times *nominal* pressure), but only about 170 s to reach the maximum pressure allowed for the RHR lines (1.9 MPa overpressure). However, if at least one of the PORV valves in the pressurizer opens, or the RHR relief valve (if this system is not isolated), the pressure can be kept within the limits, because the response of these valves is much faster than the rate of pressure increase.

5. Summary

The main conclusion from the analyses presented in this paper is that the danger of a large pressure spike at the beginning of the thermal expansion shutdown scenario that could threaten the integrity of a cold RCS or of the RHR lines (if the RHR system is not isolated) seems to be unlikely. The results obtained with the RCS completely full or with the pressurizer half empty showed that the pressure gradients due to the ther-

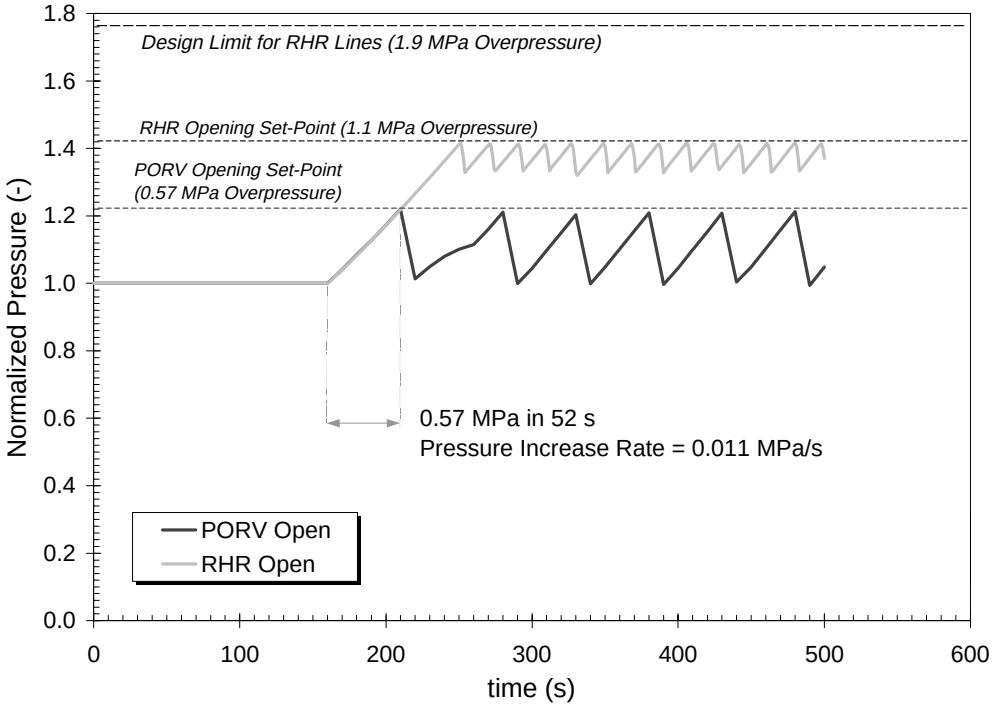

Fig. 17 RCS initially full (RCS normalized pressure and initial seconds)

mal expansion of the RCS inventory are much slower than the opening speed of both the pressurizer PORV and RHR relief valve. These valves can, venting at a minimum mass flow rate for the conditions of the scenario, maintain the RCS pressure below their opening set-points while the RCS remains subcooled.

For the normalized (with respect to the total RCS mass) valve mass flow rates given, the normalized decay heat level (relative to full power) and the pressure safety limits for the RCS and RHR lines (in terms of overpressure above the pressure at the beginning of the scenario), the valves' venting capacities provide a lower bound for the time window for operator action to restore decay heat removal capability of at least 2.6 h. After this time, the majority of the RCS reaches saturation and active vapor formation occurs. Then, the expansion of the saturated fluid exceeds the valves flow capacity and causes the RCS pressure to increase above the valves' opening set-point. This indicates that the minimum venting capacity of the valves is not sufficient to prevent the RCS pressure from increasing further unless additional pressure relieving measures are taken by the operator. Nevertheless, with the continued loss of RCS inventory though the permanently open relief valves (PORV or RHR's) and vapor formation in many locations of the RCS (especially in core and upper plenum), core uncovery and fuel damage could become the main safety concern in such an scenario.

An interesting conclusion to be drawn from these studies is that, in all cases, the RCS pressure can be kept below the pressure safety limits when just one pressurizer PORV or the RHR relief valve is activated. Regardless of the state of the RCS at the beginning of the transient, full or with the pressurizer at half level, the time window for operator action to restore decay heat removal capability before the RCS pressure increases above the valves' opening set-points depends primarily on the initial subcooling of the RCS; the higher the subcooling, the longer the time window, since the relief valves can maintain the RCS pressure below the safety limits while it remains subcooled. A significant implication, therefore, is that operator action to restore decay heat removal capability in order to reduce RCS pressure becomes even more important once active boiling appears in the RCS. After this happens, if the operators try to reduce the RCS pressure increase by venting more RCS inventory through the opening of additional relief valves (the two additional pressurizer PORVs or both the PORV and the RHR relief valve at the same time), then an excessive voiding of the core could result. Thus, restoring decay heat removal capability without further loss of RCS inventory may be the best option to consider in order to maintain RCS pressure below safety limits after the RCS subcooling has disappeared and active vapor formation occurs in the RCS. Further studies are required to clarify these aspects. A further measure that might be considered is to depressurise the steam generator as this would increase the primary side energy loss without loss of inventory.

Finally, it is worth noting that the current best estimate analysis of this scenario with RETRAN-3D permitted the simulation of the temperature distribution within the RCS. This was especially important to predict the locations of active boiling and the effect on the RCS pressure after some of the RCS regions reached saturation conditions and before the entire inventory did, and to predict a more accurate, shorter "time window" for operator remedial action than that estimated using the assumption of uniform primary temperature distribution.

IV. General Conclusions

The purpose of the work presented in this paper is to provide examples of the applicability of the best estimate (BE) code RETRAN-3D to both PWRs and BWRs currently operating in Switzerland, by means of in-depth assessment of the code results for two different kinds of scenarios, an operational transient (BWR/6) and a "beyond-design-basis" event (2-loop PWR). The transients analysed were selected (a) because of the importance of code applications to BWR operational transients without SCRAM with the power being controlled by control rod insertion and the system behavior depending on the specific characteristics of the plant studied (incorporated in the full model), and (b) because of the novel application of RETRAN-3D to PWR shutdown safety analysis.

On the basis of the results of the analyses reported, it has been shown that RETRAN-3D is capable of accurately simulating plant transients which require a full model of, not only the system thermal hydraulics, but also the core reactor kinetics and plant control and protection systems and their common interactions to determine plant response. In addition, the application of the code to a "beyond design basis" shutdown thermal expansion transient has demonstrated the advantages offered by a BE approach to accurately predict the "time window" for operator remedial action, and the applicability of RETRAN-3D to a range of PWR shutdown scenarios.

Acknowledgements

This research was partly funded by the Swiss Federal Nuclear Safety Inspectorate HSK (Hauptabteilung für die Sicherheit der Kernanlagen) and the Swiss Federal Office of Energy BFE (Bundesamt für Energie). The authors would like to thank L. Nechvatal for his support in the shutdown scenario analysis.

References

1) M. Paulsen, C. E. Peterson, J. H. McFadden, G. C. Gose, J. G. Shattford., *RETRAN-3D A Program for Transient Thermal-hydraulic Analysis of Complex Fluid Systems*, EPRI Report NP-7450, Vol. 1, (1996).
2) R. Macian, P. Cebull, M. Paulsen, P. Coddington, "Implementation of an Improved Interfacial Mass and Energy Transfer Model in RETRAN-3D," *Nucl. Technol.*, **128**, 139–152, (1999).
3) D. Maier, P. Coddington, "Evaluation of the slip options in RETRAN-3D," *Nucl. Technol.*, **128**, 153–168 (1999).
4) P. Coddington, Y. Aounallah, D. Maier, D. Reehda, "Assessment of the subcooled boiling models in RETRAN-3D and TRAC-BF1 against rod bundle and subchannel data," *Proc. NURETH-9 CD-ROM*, San Francisco, CA, (1999).
5) R. Macian, Y. Aounallah, P. Coddington, R. Stangroom, "Assessment of RETRAN-3D and VIPRE-02 void prediction against experimental transient data," *Proc. ICONE8 CD-ROM*, (2000).
6) R. Macian, P. Coddington, "Assessment of RETRAN-3D against experimental loss of coolant accident scenarios," *Proc. ICONE8 CD-ROM*, (2000).
7) H. Eitschberger, Kernkraftwerk Leibstadt AG, CH-5325 Leibstadt, Switzerland, Private communication, (1995).
8) H. Ferroukhi, P. Coddington, "Analysis of the NEACRP/NEA-NSC 3-D PWR core transient benchmarks using the CORETRAN and RETRAN-3D codes," *Proc. ICONE9 CD-ROM*, Nice, France, (2001).
9) J. T. Cronin, *SLICK. SIMULATE-3 Linking for Core Kinetics*, Studsvik Report SOA-95/20, (1995).
10) J. T. Cronin, K. S. Smith, D. M. Ver Plank, *SIMULATE-3 Methodology*, Studsvik Report/SOA-95/18, (1995).
11) J. T. Cronin, K. S. Smith, "Homogenization and functionalization of one-dimensional cross sections for RETRAN," *Nucl. Technol.*, **100**, 174–183, (1992).
12) E. T. Beaumont, *et al*., "RETRAN Benchmarks of LaSalle Units 1 and 2 Start-up Tests," Paper 12, *Proc. Eight RETRAN Int. Conf.*, EPRI Report TR-106038, (1996).
13) M. Mori, *et al*., "Verification and validation of RETRAN-03 by analytical and experience of simulating BWR plant," Paper 6, *Proc. Eighth RETRAN Int. Conf.*, EPRI Report EPRI TR-106038, (1996).
14) M. Khatib-Rahbar, "Success Criteria Analysis for Loss of RHR Cooling during Cold Shutdown Model of Operation," Calculation Note, Energy Research Inc., Rockville, MA 20847, USA, (1998).
15) ANS Standard Committee Working Group ANS-5.1, *American National Standard for Decay Heat Power in LWR*, ANSI/ANS-5.1, (1979).